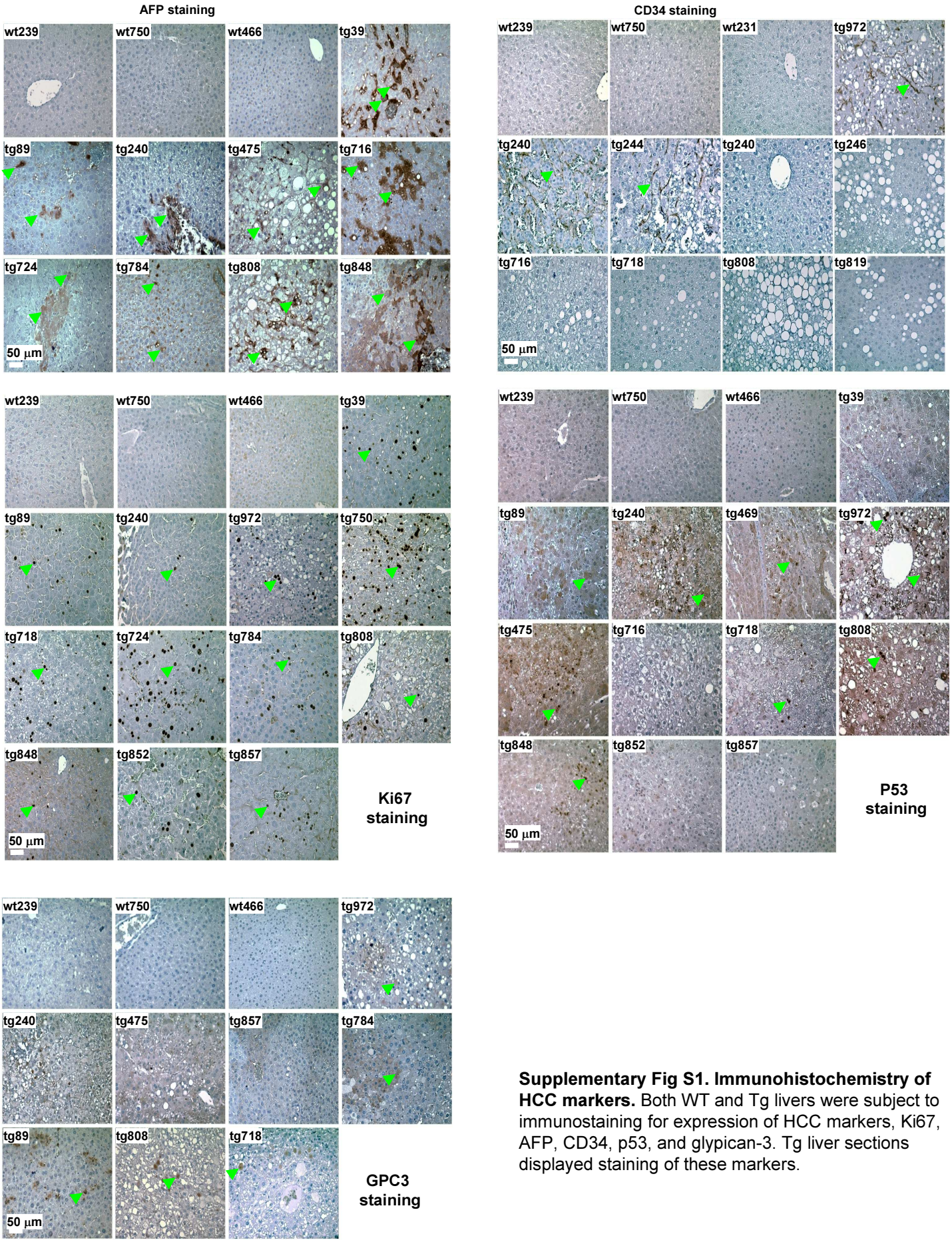

Supplementary Fig S1. Immunohistochemistry of HCC markers. Both WT and Tg livers were subject to immunostaining for expression of HCC markers, Ki67, AFP, CD34, p53, and glypican-3. Tg liver sections displayed staining of these markers.

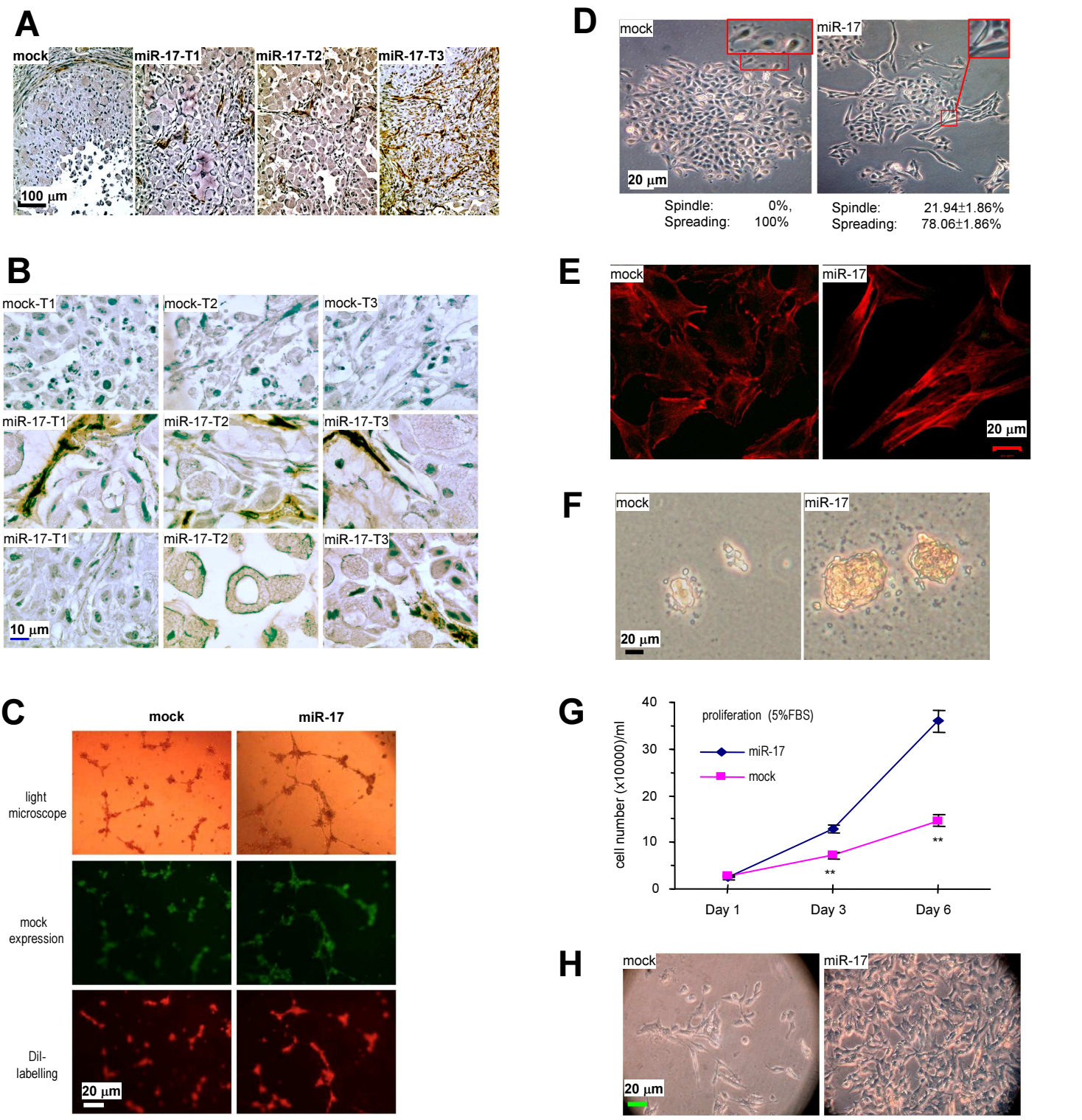

Supplementary Fig S2. Roles of miR-17 in angiogenesis and cell activities. (**A**) Tumor sections were subject to immunohistochemistry probed with anti-CD34 antibody. Expression of miR-17 construct elevated the amount of blood vessels. (**B**) Both mock- and miR-17 tumor sections were probed with anti-CD34 antibody. Blood vessels were detected in miR-17 tumors but not in mock tumors. Extensive cell death could be seen in the mock tumors but not in the miR-17 tumors. (**C**) The miR-17- and mock-transfected cells were mixed with endothelial cells YPEN, which were pre-stained with DiI dye, and inoculated in Matrigel, followed by examination of tube formation. Larger complexes and longer tubes were formed when YPEN cells were mixed with the miR-17-expressing cells compared with the mock-transfected cells. (**D**) Cell elongation was detected in the miR-17-transfected HepG2 cells as compared with mock-transfected cells. The number of spindle and spreading cells were counted and provided below the cell pictures. (**E**) The cells were also probed with anti-b-actin antibody followed by confocal microscopic examination. The miR-17-cells displayed elongated actin cytoskeleton. (**F**) Both mock- and miR-17-transfected HepG2 cells were cultured in soft agarose gel. Larger colonies were formed by miR-17-overexpressed cells. (**G**) The cells were maintained in 5% serum containing medium and the number of cells was counted on days 1, 3, and 6 to determine cell proliferation rates. MiR-17-transfected cells proliferated faster than the control cells. (**H**) Cells were maintained in serum-free conditions. Cell survival was monitored with a fluorescent microscope. Transfection with miR-17 enhanced cell survival.

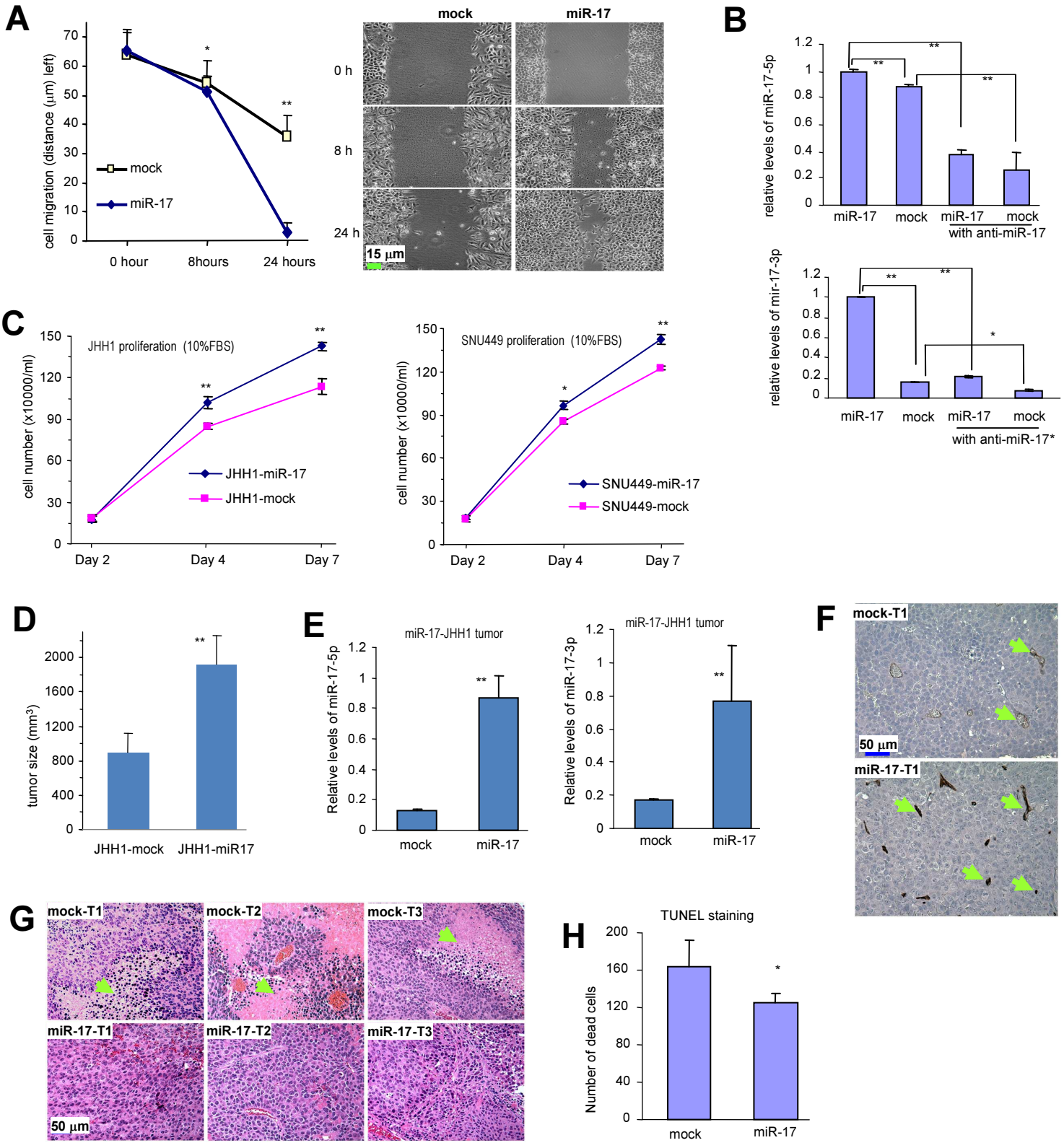

Supplementary Fig S3. Effects of miR-17 on JHH-l and SNU449 cell proliferation and tumor growth. (**A**) Left, cells were cultured for migration assay. Cells expressing miR-17 showed higher motility than the controls. Right, typical photos of cell migration are shown. (**B**) Cells were transfected with or without antisense oligos against miR-17-5p or miR-17-3p. The levels of miR-17-5p (upper) and miR-17-3p (lower) were analyzed by real-time PCR. Transfection with antisense oligos decreased miR-17-5p and miR-17-3p levels. * $p < 0.05$, ** $p < 0.01$. **(C)** JHH1 and SNU449 cells stably transfected with miR-17 or mock were subjected to proliferation assays. Expression of miR-17 promoted cell proliferation significantly more than the mock control. (**D**) The cells were injected into nude mice for tumor growth assays. Expression of miR-17 promoted tumor growth. (**E**) Expression of miR-17-5p and miR-17-3p was confirmed by real-time PCR. (**F**) Tumors sections were probed for blood vessel formation using anti-CD34 antibody. The mock-tumors showed weaker and less staining than the miR-17-tumors. (**G**) The tumor sections were also subjected to H&E staining. The tumors formed by the mock-JHHl cells displayed extensive cell death (arrows), which is less obvious in the miR-17-tumors. (**H**) Apoptotic cells in the tumor sections were analyzed by TUNEL staining. The dead cells were counted per field. Expression of miR-17 reduced tumor cell death.

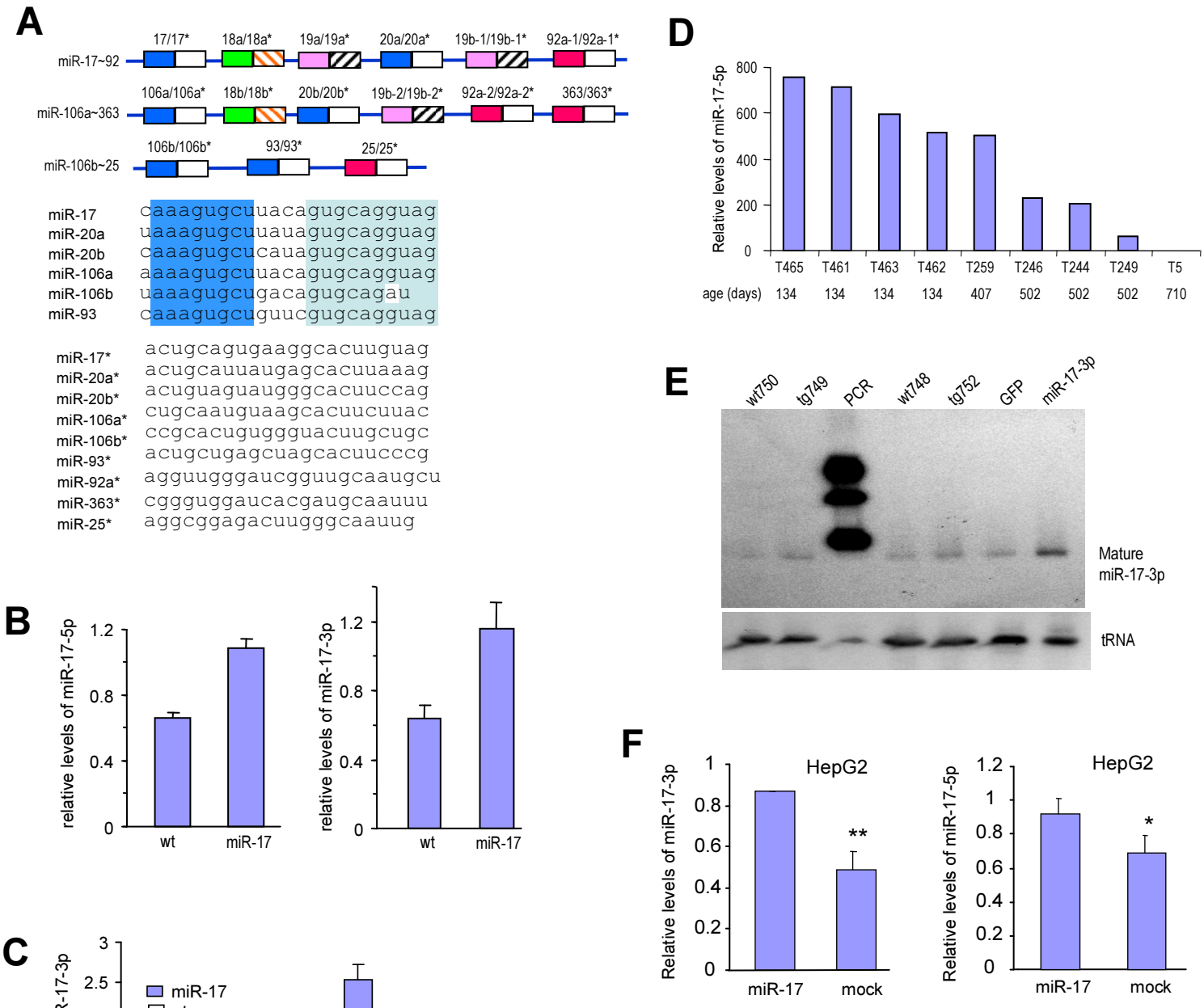

Supplementary Fig S4. Analysis of miR-17 expression in the transgenic mice. (**A**) Upper, clusters of miR-17-92, miR-106a-363 and miR-106b-25. Middle, sequence comparison of miR17 with other members harbouring the same seed sequences (highlighted). Lower, comparison of miR17-3p (miR-17*) with other miRNA* sequences in the cluster. (**B**) Expression of mature miR-17-5p and miR-17-3p were analyzed by real-time PCR using RNAs isolated from the livers of the miR-17-transgenic (Tg) and wild-type (WT) mice as indicated. Both miR-17-5p and miR-17-3p were comparably up-regulated (n = 3 PCRs. Data are mean ± s.d., * $p < 0.05$, ** $p < 0.01$.) (**C**) Expression of miR-17-5p and miR-17-3p were analyzed in miR-17 transgenic or wildtype livers, kidneys, hearts, and lungs. Both miR-17-5p and miR-17-3p were up regulated (n = 3 PCRs. Data are mean ± s.d.) (**D**) Real-time PCR analysis of miR-17-5p expression in the livers from animals of different age. (**E**) Northern blot analysis was used to detect the expression levels of miR-17-3p in HepG2 stably transfected cells, WT and Tg livers. (**F**) Expression of miR-17-5p and miR-17-3p were analyzed in HepG2 cells stably transfected with miR-17 or mock. Both miR-17-5p and miR-17-3p were up regulated (n = 3 PCRs. Data are mean ± s.d.)

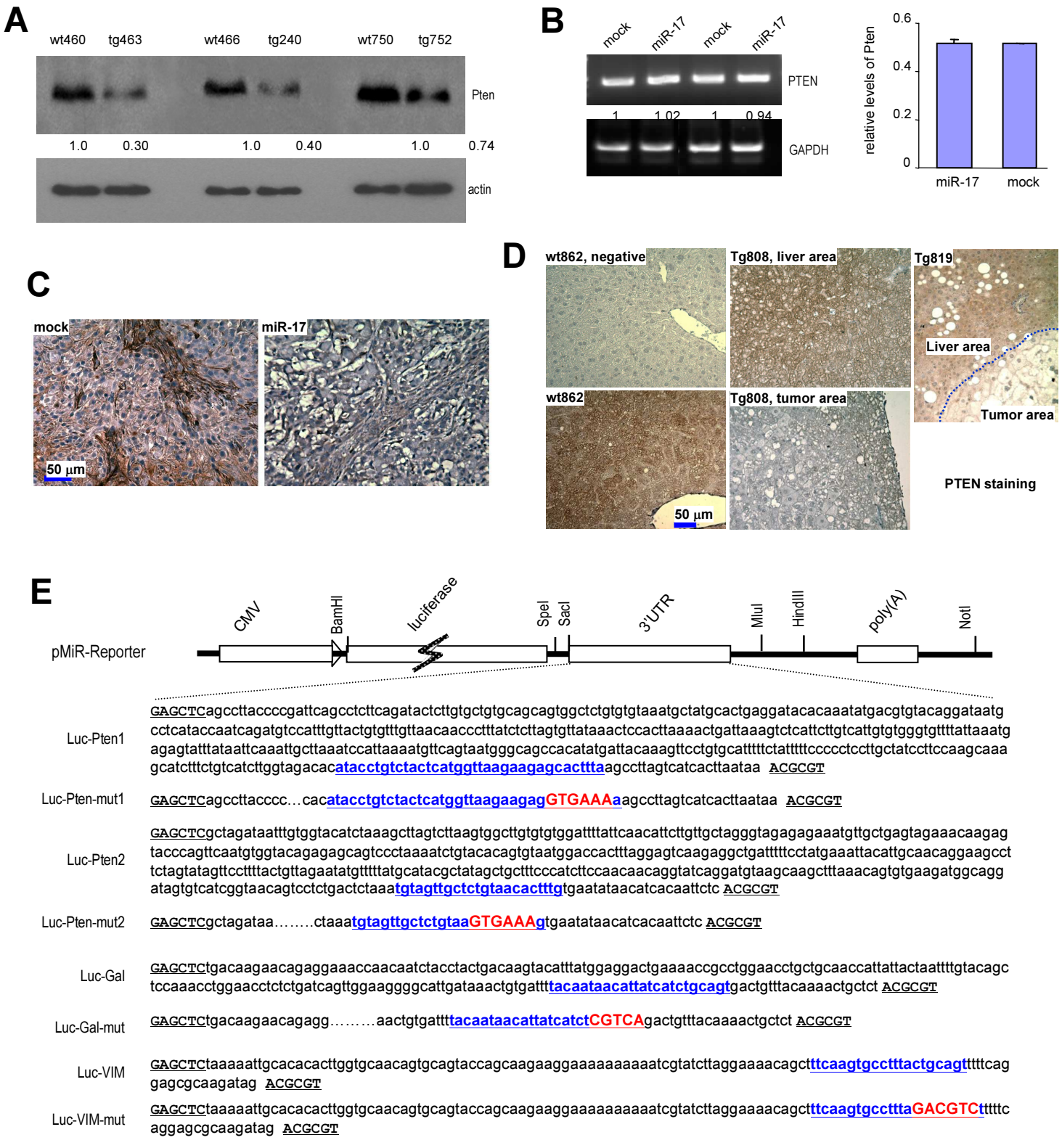

Supplementary Fig S5. MiR-17 suppressed PTEN expression. (A) PTEN protein expression was examined by western blot analysis of liver lysate from miR-17 transgenic (tg) and wild type (wt) mice and showed down-regulation of PTEN expression in the transgenic mice. (**B**) Expression of PTEN was determined with RT-PCR (left) and real-time PCR (right). No significant difference between miR-17-transfected cells and the control was detected. (**C**) The tumor sections were immunostained with anti-PTEN antibody. Tumor sections formed by the miR-17-transfected cells exhibited much lower levels of PTEN compared with the control. (**D**) Paraffin sections of miR-17 and WT livers were immunostained with an anti-PTEN antibody or the secondary antibody as a negative control. In general, PTEN staining was weaker in Tg tumors. (**E**) The 3'UTR regions of PTEN, GalNT7 and vimentin were inserted into the luciferase reporter vector pMir-Report. Mutations (red) were generated in the potential target sequence (blue).

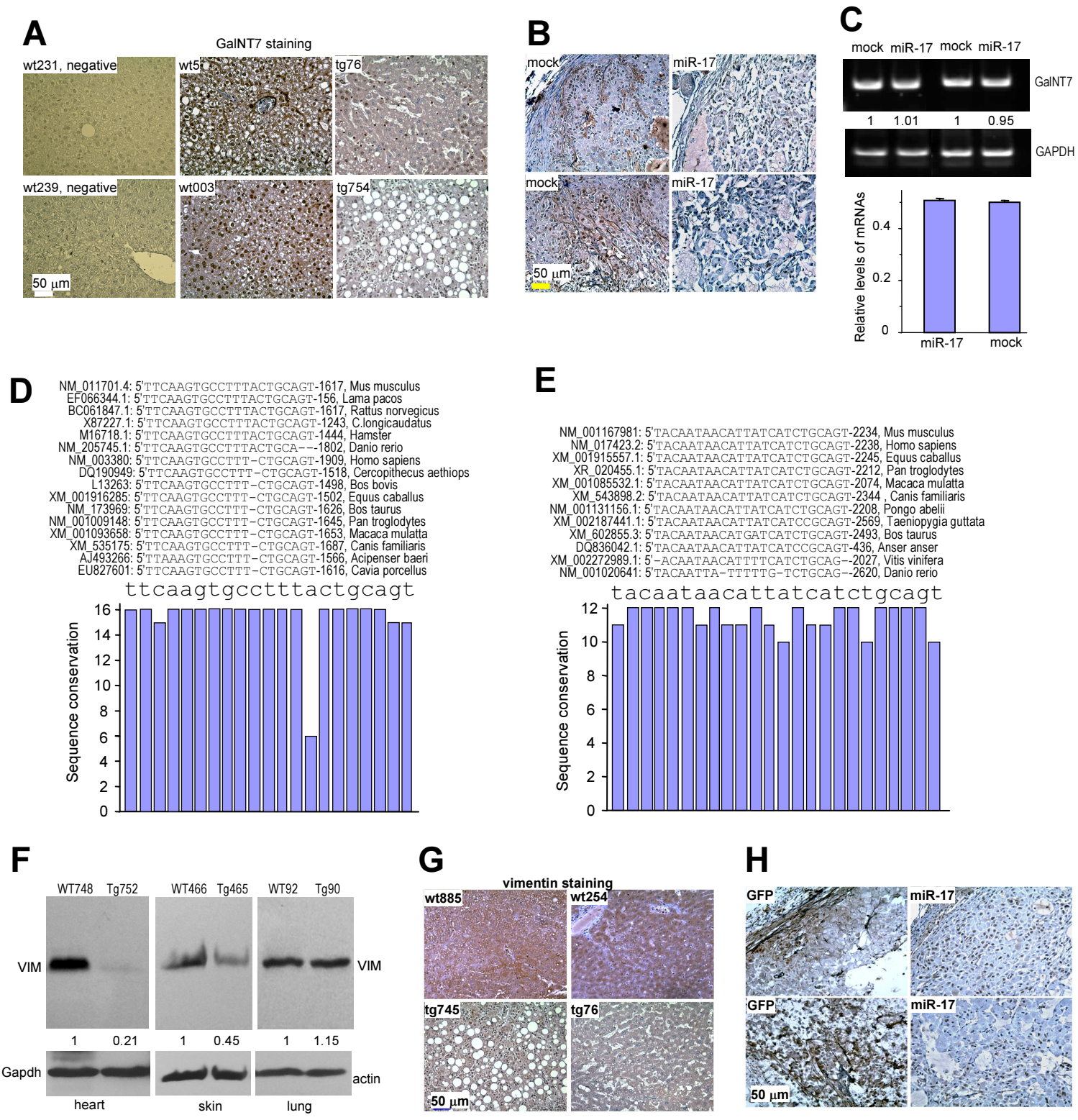

Supplementary Fig S6. MiR-17 over-expression down-regulated target levels. (**A**) Sections of Tg and WT livers were immunostained with an anti-GalNT7 antibody or with the secondary antibody as a negative control. GalNT7 staining was weaker in the Tg liver than in the WT liver. (**B**) Tumor sections were immunostained with anti-GalNT7 antibody. The miR-17 tumors exhibited lower levels of GalNT7 than mock tumors. (**C**) Expression of GalNT7 was determined with RT-PCR (upper) and real-time PCR (lower). No significant difference between miR-17-transfected cells and the control was detected. (**D**) Upper, alignment of the miR-17-3p target site in GalNT7 across different species. Lower, conservation of the sequences is shown across all species. (**E**) Top, alignment of the miR-17-3p target site in vimentin across different species. Bottom, conservation of the sequences is shown across all species. (**F**) Western blot analysis showing down-regulation of vimentin in miR-17 transgenic heart and skin. (**G**) Immunostaining for vimentin expression was performed on both Tg and WT liver sections. Tg liver exhibited lower levels of vimentin expression than the WT liver. (**H**) Tumor sections were immunostained with anti-vimentin antibody. Lower levels of vimentin were present in the miR-17 tumors than in the GFP tumors.

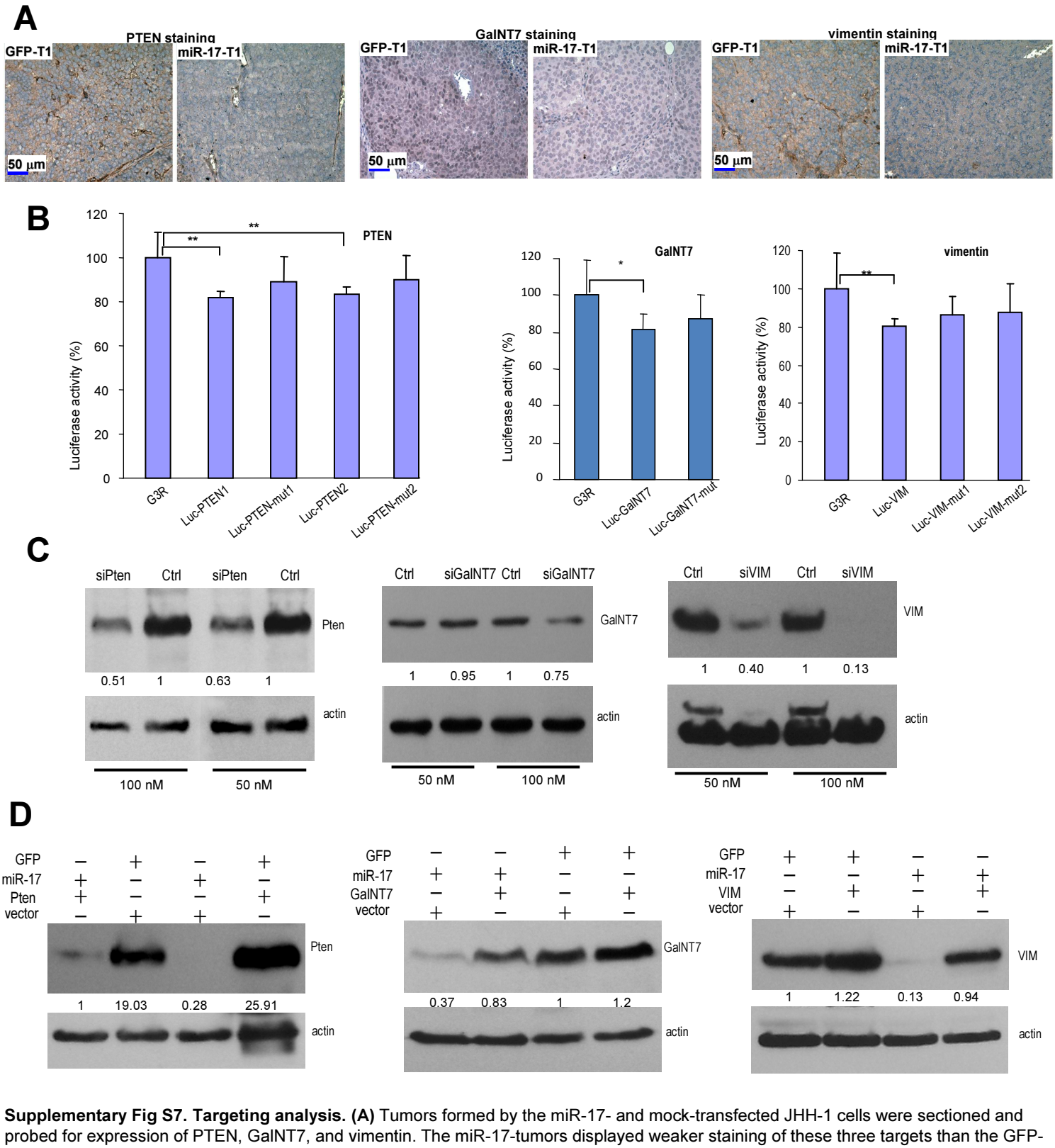

Supplementary Fig S7. Targeting analysis. (A) Tumors formed by the miR-17- and mock-transfected JHH-1 cells were sectioned and probed for expression of PTEN, GalNT7, and vimentin. The miR-17-tumors displayed weaker staining of these three targets than the GFP-tumors. **(B)** Cells were transfected with luciferase constructs harboring the 3'UTRs of PTEN, GalNT7, and vimentin to test the activities of endogenous miR-17. Controls were the constructs, which harbored the mutations of miR-17 target sites, or which contained an unrelated sequence (G3R). Luciferase activities decreased when the luciferase constructs contained the miR-17 target sites, as compared with the control constructs. **(C)** Cell lysates prepared from HepG2 cells transiently transfected with control oligos or siRNA oligos targeting PTEN, GalNT7, and vimentin were subjected to western blot analysis to confirm silencing of these proteins. Two different concentrations of oligos were used. PTEN and vimentin expressions were repressed by both concentrations of siRNA transfection (50 nM and 100 nM), while the GalNT7 was repressed when transfected with 100 nM siRNA. Staining for actin expression from the same membrane confirmed equal loading. **(D)** Both mock and miR-17-transfected HepG2 cells were transfected with (+) or without (-) control vector or expression constructs to analyze up-regulation of PTEN, GalNT7, and vimentin expression. All 3 targets were repressed when miR-17 was overexpressed in HepG2 cells. After transfecting PTEN, GalNT7 or vimentin into the cells, their respective target proteins were re-introduced in miR-17-HepG2 cells.

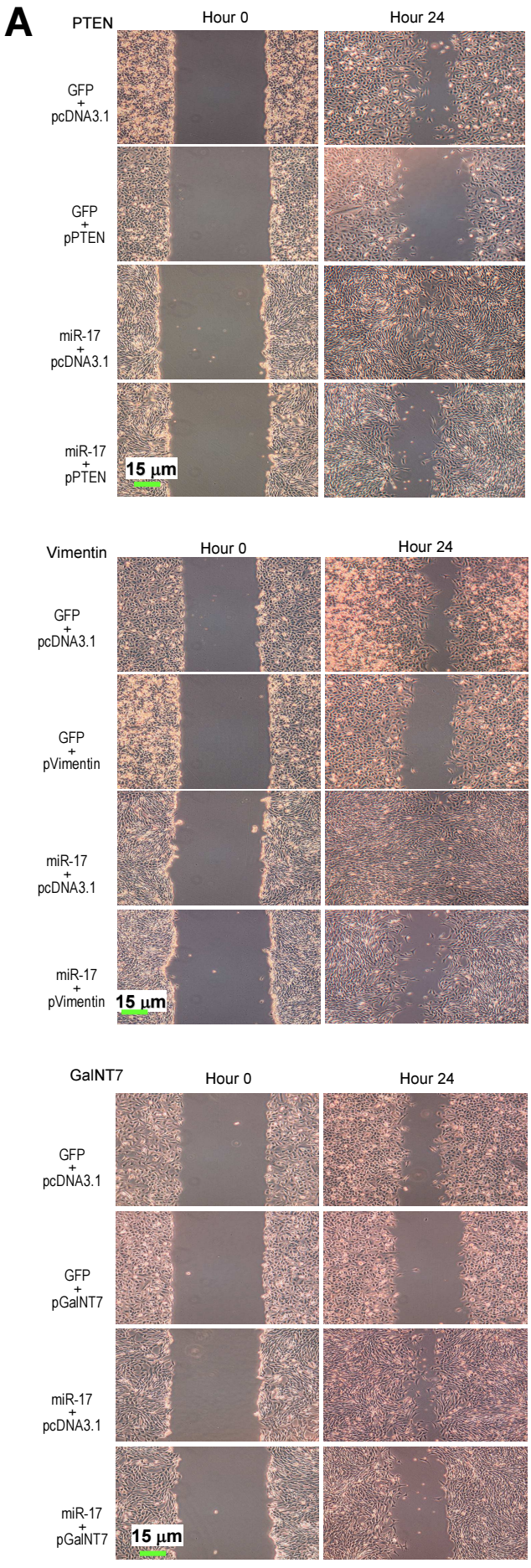

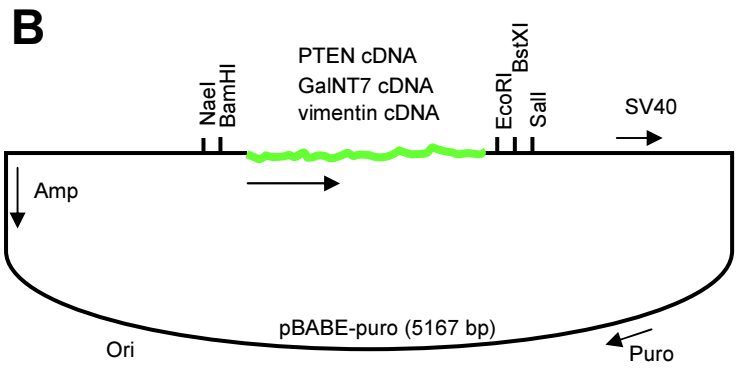

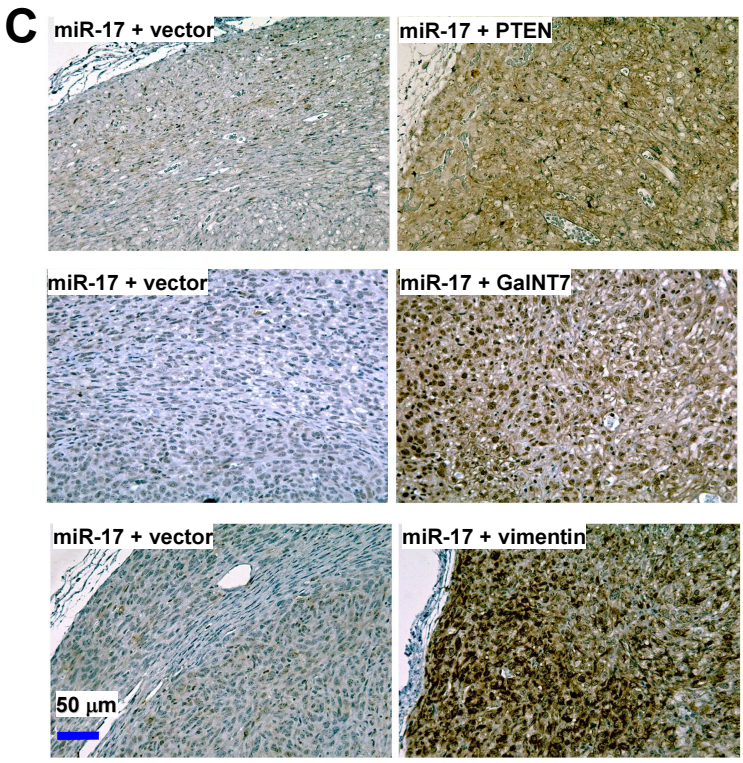

Supplementary Fig S8. Rescue experiments. (**A**) GFP- and miR-17-transfected cells were transiently transfected with expression constructs of PTEN, GalNT7, vimentin, and pcDNA3.1 vector. The cells were grown to sub-confluence and monolayers were wounded by scraping them with P200 pipette tips, washed to remove cell debris, and refilled with fresh medium. Cells were cultured for 24 hrs and fixed with 4% paraformaldehyde and photographed. (**B**) Diagram of pBABE expression constructs. (**C**) MiR-17-transfected cells were infected with retroviral vector expressing PTEN, GalNT7, or vimentin. The cells were injected into nude mice. Expression of PTEN-, GalNT7- and vimentin were confirmed by immunohistochemistry.

Supplementary Table S1 Age of mice used in the studies and tumor sizes in livers

Mice ID#	Age (days)	Tumor size (mm3)	Tumor/liver ration	Mice ID#	Age (days)	Tumor size (mm3)	Tumor/liver ration
tg5	710	-	-	tg465	134	-	-
tg7	710	-	-	wt466	134	-	-
wt7B	710	-	-	tg469	137	23.05	0.85
wt40	537	-	-	tg470	730	37.3	1.21
tg76	557	-	-	tg475	727	7.05	0.29
tg89	728	10	0.41	tg714	614	4.8	0.28
tg107	707	3.35	0.14	wt718	705	24.9	0.78
wt208	520	-	-	wt726	97	-	-
wt209	520	-	-	wt728	97	-	-
tg230	300	-	-	wt732	39	-	-
wt231	300	-	-	wt748	97	-	-
wt239	291	-	-	tg749	97	-	-
tg240	413	10.12	0.37	wt750	97	-	-
tg244	502	-	-	tg752	97	-	-
tg246	502	-	-	wt753	97	-	-
tg249	502	-	-	wt754	97	-	-
wt256	407	-	-	wt755	97	-	-
wt257	288	-	-	tg787	511	-	-
wt259	407	-	-	tg805	664	10.45	0.40
tg288	386	-	-	tg806	852	-	-
tg290	386	-	-	tg808	664	12.65	0.47
tg291	386	-	-	tg819	372	-	-
wt293	386	-	-	tg848	64	15.4	0.78
wt459	134	-	-	wt862	370	-	-
wt460	134	-	-	tg880	784	-	-
tg461	134	-	-	tg882	676	25	0.85
tg462	134	-	-	tg886	801	6.6	0.27
tg463	134	-	-	tg972	453	17.05	0.78
wt464	134	-	-	tg974	236	-	-

Supplementary Table S2. Primers used in the study

Primer name	Primer sequence
musVIM-R173p-SacI	5’cccggggagctctaaaaattgcacacacttggtgc
musVIM-R173p-MluI	5’gggcccacgcgtctatcttgcgctcctgaaaaactgc
musGalNT7VIM-R17*-SacI	5’cccggggagctctgacaagaacagaggaaaccaacaatc
musGalNT7VIM-R17*-MluI	5’gggcccacgcgtagagcagttttgtaaacagtcactgc
musPten3084-R17-SacI	5’gggagctcagccttaccccgattcagcctcttcag
musPten3084-R17-MluI	5’ccacgcgtttattaagtgatgactaaggct
chver10051-SpeI	5'gggcccactagtaatggagccacatgtatagat
chver10350-SacI	5'gggcccgagctcgaaatcacgctcaaacatctt
human-U6RNAf	5’gtgctcgcttcggcagcacatatac
Human-U6RNAr	5’aaaaatatggaacgcttcacgaatttg
Hu-Gapdh421F	5’aaggctggggctcatttgcag
Hu-Gapdh720R	5’gatgttctggagagccccgcg
EGFP981F	5’caaggacgacggcaactacaagac
EGFPC-ApaI	5’cccgggccccttgtacagctcgtccatgcc